Pore Structure Characteristics of Activated Carbon Fibers Derived from Poplar Bark Liquefaction and Their Use for Adsorption of Cu(II)

Jiahui Zhang,[a] Wenbo Zhang,[a, b,*] and Yue Zhang [a]

In this work, wood bark was liquefied to prepare activated carbon fibers, which were obtained through melt-spinning, stabilization, carbonizing, and stream activation. The effects of varying activation temperature on the pore structure and the adsorption capacity of the liquefied wood bark activated carbon fibers (LWBACFs) were studied using analysis of nitrogen adsorption-desorption isotherms and static adsorption of copper (II) ions from aqueous solution. The results indicated that higher specific surface area was obtained as the activation temperature increased. The specific surface area reached a maximum of 1962 m^2/g with an average pore diameter of approximately 2 nm. Carbonization at 200 °C played an important role in the formation of pore structure. The adsorption of copper by LWBACFs was high, with a peak of 15 mg/g. All parameters showed that LWBACFs performed well in the adsorption of micropores.

Keywords: Wood bark; Activated carbon fiber; Pore structure; Heavy metal removal; Copper ions

Contact information: a: College of Material Science and Technology; b: MOE Key Laboratory of Wooden Material Science and Application, Beijing Forestry University, Beijing 100083, P. R. China;
** Corresponding author: kmwenbo@bjfu.edu.cn*

INTRODUCTION

Wood bark, one of the most common types of biomass resources, is a forestry residue of great importance. The gross production of wood in China reached 81 million m^3 last year, of which wood bark accounted for 10%. This consumption has resulted in an increase in wood bark stock every year. Currently, wood bark is disposed of *via* burning or waste disposal, generating atmospheric pollutants harmful to the environment and to human health. This has led to a huge waste of wood bark. Wood bark contains biomass fibers with a porous capillary structure. These distinctive characteristics are advantageous to pore-forming materials such as activated carbon fiber. Activated carbon fiber is a type of multi-duty material with a preferable porous structure, large specific surface area, and stronger adsorption ability than activated carbon. In recent years, environmental pollution problems caused by heavy metal ions, which are known to be poisonous and harmful to the environment, have become a global concern. Heavy metal ions (such as cadmium, copper, and nickel) can cause serious health and environmental problems. Activated carbon fibers, with their excellent adsorption capacities, have attracted a lot of research interest as they are considered to be promising candidates for heavy metal removal. Currently, activated carbon fibers are mainly produced from polyacrylonitrile (Yusof *et al.* 2012), and other fossil material products and are widely used as absorbents in many industrial areas, especially for removal of heavy metals during the purification of

industrial wastewater. Additionally, more and more researchers are focusing on activated carbon fiber preparation from biomass materials on the basis of recycling and sustainability. As one of the economical and easily used techniques, adsorption has been used for heavy metal removal and offers several advantages, such as low cost, high removal capacity, ease of use, and flexibility in design and operation (Shawabkeh *et al.* 2002). Some sorbents such as zeolite (Sheta *et al.* 2003), yeast (Yang *et al.* 2008), and other porous materials have been applied for heavy metal removal. As of now, there have not been many studies regarding heavy metal removal using wood-based activated carbon fibers derived from waste wood bark liquefaction. From the viewpoints of waste reuse, low cost, and eco-friendly material development, such use of waste wood bark may simultaneously solve the following problems: waste disposal, minimizing emissions of toxic substances, and development of low cost biosorbents for purifying wastewater containing heavy metal ions.

In this work, LWBACFs were prepared by one-step steam activation using the previous preparation process of liquefaction, spinning, stabilization, and carbonization. The proper carbonization temperature was investigated. The effects of several characteristics such as adsorption capacities and heavy metal adsorption were also determined. The adsorption capacities were calculated *via* low-temperature nitrogen adsorption. Meanwhile, the adsorption capacity of LWBACF samples to Cu(II) in aqueous solutions were also tested. Therefore, the present work is significant with respect to the application of LWBACFs in environmental protection, the chemical industry, and other areas.

EXPERIMENTAL

Materials

All chemicals used were of analytical reagent grade. Wood bark was obtained from poplar (*Populus euramevicana* cv. 'I-214'), a widely planted, fast-growing tree in eastern China. The barks were washed with deionized water until all impurities were removed from the bark surfaces. The barks were then completely dried in an oven at 80 ±2 °C. The dried barks were then ground and screened to 60 to 80-mesh size.

Methods

Bark powder was mixed with phenol containing H_3PO_4 (10%, based on the weight of bark powder) as the reaction catalyst. The ratio of the bark/phenol was 1/4 by weight. The mixture was liquefied in a 500-mL three-neck glass flask by being held at 160 °C for 2 h with continuous stirring.

Liquefied bark was then put into a self-made spinning apparatus with hexamethylenetetramine (HMTA, 5%, based on the weight of liquefied bark). The mixture was heated from room temperature to 130 °C over 40 min with a stirring speed of 80 rpm. The temperature was held for 10 min for the spinning solution. Then, the spun filaments were continuously wound on a bobbin at 100 °C at a speed of 0.36 m/min.

The resultant precursor fibers were cured *via* soaking in a solution containing hydrochloric acid and formaldehyde (volume ratio 30:37) as the two primary components at 90 °C for 2 h (Ma and Zhao 2008, 2011). Precursor fibers were obtained after washing with deionized water and drying (at 85 °C) for 4 h.

Thereafter, precursor fibers were carbonized (at 200, 300, or 600 °C) and steam-

activated (at 700, 800, or 900 °C) under an inert nitrogen atmosphere at a heating rate of 4 °C/min from room temperature to activation temperature in a single step. Then the activation process was continued for 60 min with a mixture of steam and protective gas. Using this method, the samples were carbonized and activated in a continuous heating process without a cooling period. Samples treated at different conditions were denoted by carbonized temperature-activated temperature codes, such as 200-700. In this way, samples were divided into nine groups according to the different carbonization and activation temperatures (200-700, 300-700, 600-700, 200-800, 300-800, 600-800, 200-900, 300-900, and 600-900).

The pore structure characteristics were measured with a specific surface area/pore size distribution detector (Autosorb iQ) using nitrogen adsorption and desorption isotherms at 77 K over a wide range of relative pressure. Before the measurements, all samples were outgassed at 300 °C for 3 h with highly pure nitrogen (99.99%). The specific surface area was calculated using the Brunauer-Emmett-Teller (BET) method (Brunauer *et al*. 1938). The micropore volume, micropore area, mesopore volume, and mesopore area were estimated using the *t*-plot method (de Boer *et al*. 1966). The pore size distribution was determined using the density functional theory (DFT) (Lastoskie *et al*. 1993). The pore volume and average pore size were calculated based on the assumption that nitrogen filled the sample pores at a relative pressure of 0.995.

Heavy metal adsorption equilibrium experiments were conducted to determine the adsorption capacity of Cu(II) on LWBACFs as a function of the initial concentration of Cu (II) ions in solution. Samples were triturated and screened to size of 40-mesh. The LWBACF samples were then put into 100-mL solutions containing Cu(II) ions at concentrations of 2.5, 5, 10, 15, 25, and 50 mg/L with an adsorbent dose of 0.25 g. The mixed solutions were shaken with a rotational speed of 200 rpm after the pH was adjusted to 5.0 by adding a few drops of 1 M HCl or NaOH solutions. The pH was selected based on preliminary data. The concentrations of Cu(II) ions in the solutions were determined after continuous shaking for 120 min. All experiments were carried out at room temperature (25 ± 2 °C). The copper adsorption capacity of samples was investigated with an atomic absorption spectrophotometer (Varian AA220). During the adsorption, a relative equilibrium was established between the adsorbed metal ions and unadsorbed metal ions in solution. The adsorption capacity of Cu (II) ions were calculated by Eq. 1,

$$Q = (C_0\text{-}C_e)V/M \quad (1)$$

where V(L) is the volume of solutions and M(g) is the weight of adsorbent.

RESULTS AND DISCUSSION

Pore Structure

The curves presented in Fig. 1 are the nitrogen adsorption-desorption isotherms for LWBACFs carbonized at 200, 300, and 600 °C at different activation temperatures. According to the IUPAC classification, all the isotherms exhibit type I characteristics, indicating the presence of micropores.

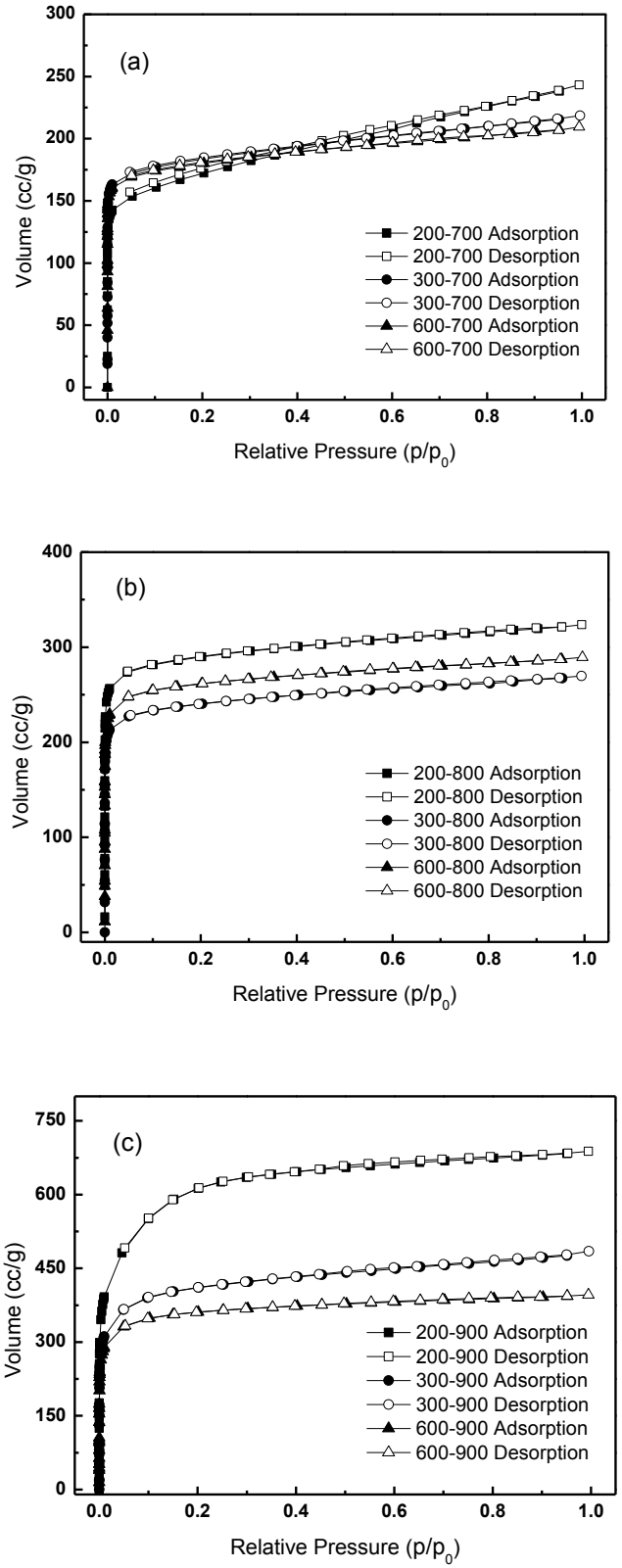

Fig. 1. Nitrogen adsorption-desorption isotherms of LWBACFs: (a) effect of carbonization temperature at 700 °C; (b) effect of carbonization temperature at 800 °C; and (c) effect of carbonization temperature at 900 °C

It is worth noting that the isotherms also exhibited some characteristics of type II and type IV isotherms (the volume still increased with the increase in relative pressure), which indicates the existence of mesopores (Lee *et al*. 2003; Zhang *et al*. 2008). An increase in the samples' nitrogen adsorption capacity occurred with decreasing carbonization temperature and increasing activation temperature. For example, the adsorbed volume of the 200-700 sample at the relative pressure of around 0.99 was only about 209 cc/g, while that of the 600-900 sample was a much-improved 688 cc/g.

The pore size distributions (PSDs) of LWBACFs with different activation temperatures are presented in Fig. 2. The data were obtained using the DFT method. It can be seen that the PSDs of LWBACFs activated at 700 to 900 °C were narrow and were mostly between 0.5 and 2 nm, a good distribution of micropores. The numbers of mesopores are rather small (mainly distributed at 2 to 25 nm with a few discernible peaks, not shown completely in the figure) and gradually decreased with increasing activation time. Carbonization did not play an important role in the pore size distribution. Figure 2 shows that the micropore size tended to increase with increasing activation temperature. This might be because higher temperatures removed active amorphous atoms and unsaturated carbon atoms from the edges of the micrographitic walls and partially gasified the micropore walls, thereby increasing the size of the micropores (Ishii *et al*. 1997).

Pore characteristics of LWBACF samples are shown in Table 1. The maximum BET specific surface area was 1962 m^2/g, which is higher than that of other commercial ACFs (Shen *et al*. 2011; Sun *et al*. 2011). The total pore volumes of samples varied from 0.324 to 1.064 cm^3/g. Both parameters increased with increasing activation temperature. Meanwhile, carbonization temperatures around 200 °C play an important role in the follow-up formation of pore structure because of the relatively higher specific surface area than other carbonization temperatures. This may relate to the severe pyrolysis and slow coking of the carbon-rich raw materials. High temperature is helpful for promoting the carbon oxidation reaction conversion rate in activation process, which could improve of specific surface area, as the 200-900 sample showed. S_{micro} and V_{micro} values were all much higher than S_{meso} and V_{meso}, suggesting that the samples had abundant micropores. The average pore diameter changed only slightly with variations of the carbonization and activation temperatures, ranging from the 2.169 to 2.743 nm.

Table 1. Pore Characteristics of LWBACF Samples

Sample	Specific surface area (m^2/g)			Pore volume (cm^3/g)			Average pore diameter (nm)	Micropore ratio (%)
	S_{BET}	S_{micro}	S_{meso}	V_{total}	V_{micro}	V_{meso}		V_{micro}/V_{total}
200-700	549	397	152	0.376	0.209	0.167	2.743	55.585
300-700	565	489	76	0.338	0.257	0.081	2.393	76.036
600-700	554	493	61	0.324	0.259	0.065	2.340	79.938
200-800	886	813	73	0.501	0.424	0.077	2.260	84.631
300-800	734	673	61	0.417	0.352	0.065	2.275	84.412
600-800	798	738	60	0.448	0.385	0.063	2.243	85.938
200-900	1962	1822	140	1.064	0.922	0.142	2.169	86.654
300-900	1274	1126	148	0.750	0.586	0.164	2.355	78.133
600-900	1105	1030	75	0.613	0.535	0.078	2.217	87.276

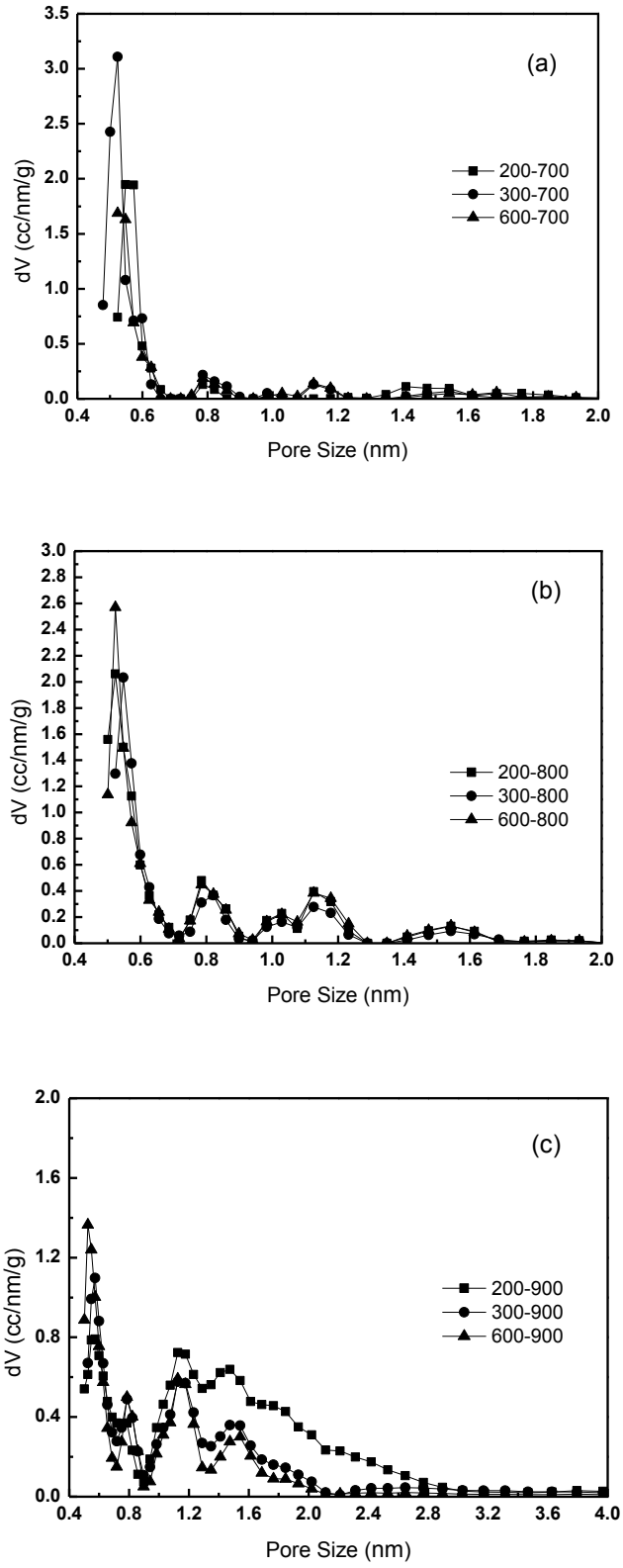

Fig. 2. Pore size distributions of the LWBACF samples: (a) effect of carbonization temperature at 700 °C; (b) effect of carbonization temperature at 800 °C; and (c) effect of carbonization temperature at 900 °C

Attractive forces exist on the surfaces of fibers. Greater surface area corresponds to greater adsorption capacity. This is more effective for fibers and adsorbates in the same order of magnitude, which shows that a microporous structure has a good adsorption capacity for gases.

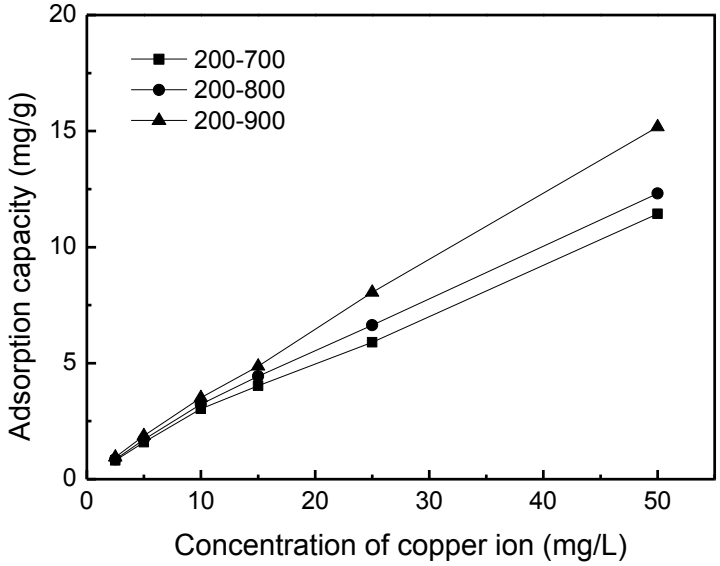

Fig. 3. Cu^{2+} adsorption capacity of LWBACF

Heavy Metal Adsorption

The effects of initial concentration on the adsorption efficiency of Cu(II) ions absorbed by LWBACFs are shown in Fig. 3. The 200-X samples were chosen because of their excellent pore structures and capacities. The removal rates were calculated using Eq. 1.

As shown in the figure, the amount of Cu(II) adsorbed ions by the samples increased linearly with increasing initial Cu(II) ion concentration, indicating a good overall adsorption capacity for Cu(II) ions. The adsorption capacity reached 15 mg/g, a higher adsorption capacity than other adsorbents as reported in previous studies (Rajvinder *et al.* 2013; Witek-Krowiak 2013). The pore diameters of LWBACF samples, in which micropores were dominant, were within a similar order of magnitude as Cu(II) ion (with an ionic radius of about 0.072 nm), resulting in easier adsorption of Cu(II) ions. The results showed that LWBACFs are a promising sorbent for low-concentration heavy metal solutions.

From the viewpoints of waste reuse, low cost, and eco-friendly material development, such use of waste wood bark may simultaneously solve the following problems during trial stages: waste disposal, emissions of toxic substances, and low cost biosorbent development for purifying wastewater containing heavy metal ions. The experimental results are considered to be an important step towards practical production in the subsequent progress of research. In this way, the advantages of ACFs compared with other activated carbon varieties can be demonstrated by full-scale operation.

CONCLUSIONS

1. Liquefied wood bark activated carbon fibers (LWBACFs) were prepared through sequential carbonization and steam activation. Temperatures ranging from 800 to 900 °C were ideal during the activation reaction stage and caused significant pore structure changes.
2. The nitrogen adsorption-desorption isotherms of LWBACFs were Type I. This indicates a good presence of micropores.
3. The specific surface area and pore volume increased with increasing activation temperature. The maximum specific surface area was 1962 m^2/g following carbonization at 200 °C and activation at 900 °C. Meanwhile, the process generated similar distributions of pore size, which indicated less of an impact on the formation of pore size.
4. Carbonization temperature had important effects on pore structure formation. With increasing carbonization temperature, the micropore ratio increased with decreasing specific surface area. The maximum micropore ratio was 87.3% for the 600-900 sample, whereas the minimum was 55.6% for the 200-900 sample.
5. The LWBACFs showed a high adsorption capacity for Cu(II). The highest adsorption capacity was 15.2 mg/g with the 200-900 LWBACF sample.

ACKNOWLEDGMENTS

The authors are grateful for the financial support of the state forestry administration of the People's Republic of China through the 948 project (No. 2013-4-04).

REFERENCES CITED

Brunauer, S., Emmett, P. H., and Teller, E. (1938). "Adsorption of gases in multimolecular layers," *J. Am. Chem. Soc.* 60(2), 309-319. DOI: 10.1021/ja01269a023

de Boer, J. H., Lippens, B. C., Linsen, B. G., Broekhoff, J. C. P., van den Heuvel, A., and Osinga, T. J. (1966). "T-curve of multimolecular N_2-adsorption," *J. Colloid Interf. Sci.* 21(4), 405-414. DOI: 10.1016/0095-8522(66)90006-7

Ishii, C., Suzuki, T., Shindo, N., and Kaneko, K. (1997). "Structural characterization of heat-treated activated carbon fibers," *J. Porous Mat.* 4(3), 181-186. DOI: 10.1023/A:1009614901091

Lastoskie, C., Gubbins, K. E., and Quirke, N. (1993). "Pore size distribution analysis of microporous carbons: A density functional theory approach," *J. Phys. Chem.* 97(18), 4786-4796. DOI: 10.1021/j100120a035

Lee, Y. S., Basova, Y. V., Edie, D. D., Reid, L. K., Newcombe, S. R., and Ryu, S. K. (2003). "Preparation and characterization of trilobal activated carbon fibers," *Carbon* 41(13), 2573-2584. DOI: 10.1016/S0008-6223(03)00376-2

Ma, X., and Zhao, G. (2008). "Structure and performance of fibers prepared from liquefied wood in phenol," *Fiber. Polym.* 9(4), 405-409. DOI: 10.1007/s12221-008-0065-6

Ma, X., and Zhao, G. (2011). "Variations in the microstructure of carbon fibers prepared from liquefied wood during carbonization," *J. Appl. Polym. Sci.* 121(6), 3525-3530. DOI: 10.1002/app.34142

Rajvinder, K., Joginder, S., Rajshree, K., Swarantjit, S. C., and Amjad, A. (2013). "Batch sorption dynamics, kinetics and equilibrium studies of Cr (VI), Ni (II) and Cu (II)from aqueous pahse using agricultural residues," *Appl. Water Sci.* 3(1), 207-218. DOI: 10.1007/s13201-012-0073-y

Shawabkeh, R., Rockstraw, D., and Bhada, R. (2002). "Copper and strontium adsorption by a novel carbon material manufactured from pecan shells," *Carbon* 40(5), 781-786. DOI: 10.1016/S0008-6223(01)00198-1

Shen, Q., Zhang, T., Zhang, W., Chen, S., and Mezgebe, M. (2011). "Lignin-based activated carbon fibers and controllable pore size and properties," *J. Appl. Polym. Sci.* 121, 989-994. DOI: 10.1002/app.33701

Sheta, A., Falatah, A., Al Sewailem, M., Khaled, E., and Sallam, A. (2003). "Sorption characteristics of zinc and iron by natural zeolite and bentonite," *Micro. Meso. Mater.* 61(1-3), 127-136. DOI: 10.1016/S1387-1811(03)00360-3

Sun, Y., Yang, G., Zhang, J., Wang, Y., and Yao, M. (2011). "Activated carbon preparation from lignin by H_3PO_4 activation and its application to gas separation," *Chem. Eng. Technol.* 35(2), 309-316. DOI: 10.1002/ceat.201100309

Witek-Krowiak, A. (2013). "Application of beech sawdust for removal of heavy metals from water: biosorption and desorption studies," *Eur. J. Wood Prod.* 71(2), 227-236. DOI: 10.1007/s00107-013-0673-8

Yang, H., Xu, R., Xue, X., Li, F., and Liu, G. (2008). "Hybrid surfactant-templated mesoporous silica formed in ethanol and its application for heavy metal removal," *J. Hazard Mater.* 152(2), 690-698. DOI: 10.1016/j.jhazmat.2007.07.060

Yusof, N., Ismail, A. F., Rana, D., and Matsuura, T. (2012). "Effects of the activation temperature on the polyacrylonitrile/acrylamide-based activated carbon fibers," *Mater. Lett.* 82, 16-18. DOI: 10.1016/j.matlet.2012.04.150

Zhang, S. J., Feng, H. M., Wang, J. P., and Yu, H. Q. (2008). "Structure evolution and optimization in the fabrication of PVA-based activated carbon fibers," *J. Colloid Interf. Sci.* 321(1), 96-102. DOI: 10.1016/j.jcis.2008.01.012

Article submitted: September 16, 2014; Peer review completed: November 9, 2014; Revised version received and accepted: November 18, 2014; Published: November 26, 2014.